J Sol-Gel Sci Technol (2016) 77:437–445
DOI 10.1007/s10971-015-3872-4

ORIGINAL PAPER

Microstructure and transport properties of biocompatible silica hydrogels

Mercedes Perullini[1] · Nathanael Levinson[1] · Matías Jobbágy[1] · Sara A. Bilmes[1]

Received: 23 July 2015 / Accepted: 18 September 2015 / Published online: 29 September 2015

Abstract Silica matrices are suitable for encapsulation of biomolecules and microorganisms to build bioactive functional materials. For many applications of these host–guest systems, the performance highly depends on the tuning of transport properties. Here we analyze the microstructure of silica hydrogels from small-angle X-ray scattering (SAXS) experiments and its correlation with their transport properties evaluated from the fitting of diffusional profiles of the cationic dye crystal violet (CV). We found a clear correlation between the microstructure parameters and the transport of CV over a wide range of synthesis conditions (SiO_2 total content from 3.6 to 9.0 % and pH of silica condensation from 4.5 to 7.5). At pH $\sim$ 6, non-monotonic changes in transport properties can be attributed to the discontinuity observed in microscopic parameters, revealing the inherent complexity of the sol–gel transition. However, regardless of the pH of synthesis and for each set of samples with a fixed silica concentration, CV apparent diffusion coefficient (D_{app}) is inversely proportional to the parameter S (related to the silica/aqueous-solution interfacial area) derived from SAXS. These results indicate that macroscopic properties cannot be easily predicted from the pH of synthesis, in particular around neutral pH that is relevant for biotechnological applications. Nonetheless, the close correlation between D_{app} and the microstructure parameters of the studied systems allows proposing a predictive value of any of these approaches toward the other.

Electronic supplementary material The online version of this article (doi:10.1007/s10971-015-3872-4) contains supplementary material, which is available to authorized users.

✉ Mercedes Perullini
mercedesp@qi.fcen.uba.ar

[1] INQUIMAE-DQIAQF, Facultad de Ciencias Exactas y Naturales, Universidad de Buenos Aires, Ciudad Universitaria, Pab. II, C1428EHA Buenos Aires, Argentina

Graphical Abstract

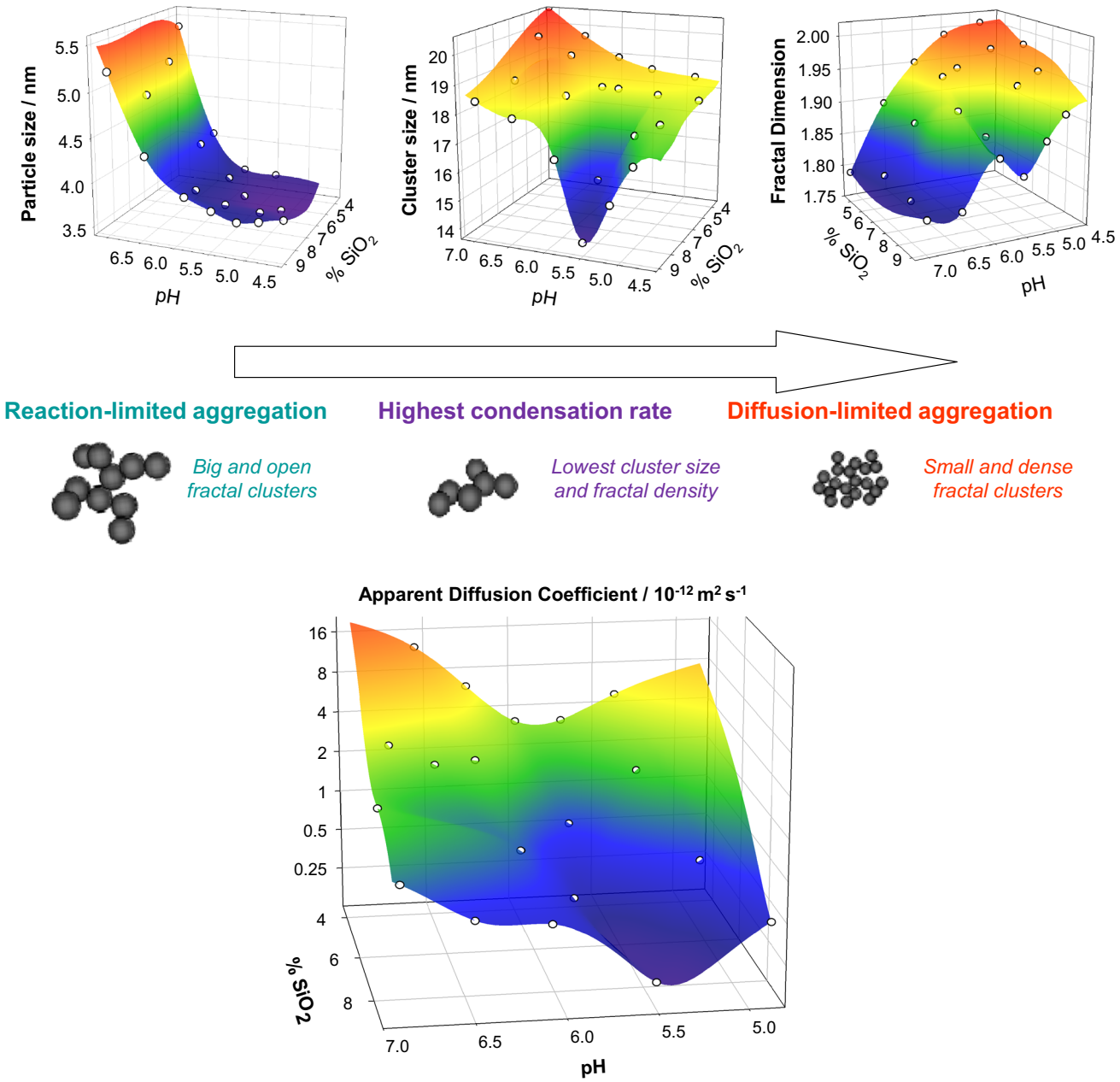

Keywords Silica hydrogels · TEOS alcohol-free route · SAXS microstructure characterization · Transport properties

1 Introduction

Sol–gel-derived silica is attracting increasing interest for the synthesis of functional materials with biological activity (MBAs) through encapsulation of enzymes, antibodies or other macromolecules [1], whole cells [2, 3] and even metazoa [4] for different applications, such as the design of biosensors [5–8], modular bioreactors [9–11], filtration devices or coatings [12–14]. The encapsulation of biologically active entities inside inorganic matrices implies an intrinsic limitation in synthesis conditions, as the overall process must evolve within biocompatible chemical constraints (pH, water activity and osmotic strength) imposed by the biological guest [15, 16]. On the other hand, some macroscopic properties of such wet gels can be desirable or even necessary. In particular, the transport of dissolved species can be critically important to ensure optimal performance of most applications. However, the optimization of transport properties must fulfill other needs, such as optical quality and mechanical resistance that require a fine control of the synthesis parameters

and a detailed characterization of their structure in the 0.1 nm–1 μm range. The meso- and microporous structures of sol–gel materials can be tuned by modifying the synthesis parameters, such as precursors nature, pH and additives, giving rise to oxide networks with well-defined porosity that are useful for the design of MBAs [17].

A traditionally used pathway for SiO_2 hydrogel formation is the catalytic polycondensation of tetraalkoxysilanes in an alcoholic environment for which extensive characterization of the process has been done [18]. However, in spite of the mild conditions of sol–gel synthesis, routes based on alkoxides as precursors present low biocompatibility [19], mainly due to the alcohol by products. A well-established modification of this procedure consists on the previous removal of the harmful alcohol generated during the synthesis [20]. These alcohol-free routes include a previous hydrolysis in acid media where water is added as a reagent and the controlled low-pressure evaporation of the alcohol that results as a byproduct of the hydrolysis and condensation of alkoxide precursors immediately before the addition of the biological entity in a buffer aqueous solution at the desired pH [21].

The microstructure of silica gels has been extensively studied mainly by scattering techniques (neutrons, X-ray, light) [22]. It has been shown that silica backbone is formed by the aggregation of small particles into clusters, conforming a structure that can be assimilated to a mass fractal over intermediate sizes, smaller than the average cluster size (R_g) and larger than the mean diameter of the dense elementary particles composing the structure (a). The concept of fractal [23] is appropriate to describe a structure formed as a result of random condensation and aggregation processes. The fractal dimension (D) describes de mass distribution in the volume: $m \sim r^D$, where m is the mass and r is the distance in the D-dimensional space. Thus, the parameters a, R_g and D describe the microstructure which in turn determines the macroscopic properties of the resulting hydrogel. In a previous work, we studied the close relationship between synthesis parameters and microstructure of silica hydrogels synthesized by the TEOS-derived alcohol-free route (TAFR) as well as the correlation of microstructure and optical properties of these matrices [24]. However, by further analysis of the SAXS scattering curves, a parameter (S) related to the silica/aqueous-solution interfacial area per unit volume can be obtained. Since the diffusion of positively charged species through the aqueous pores of the matrix is coupled with adsorption on the silica surface, the transport of these molecules depends on the porosity as well as on the specific surface of the matrix.

Many devices and methods have been developed, and detailed mathematical models were proposed to study diffusion–adsorption phenomena within silica matrices. However, monitoring the transport of color moieties by digital image analysis proved to be adequate for the simultaneous determination of dye diffusion and adsorption parameters on the silica matrix [25–27].

Here we present a systematic study to establish the effect of synthesis conditions (concentration of precursors and pH of condensation reaction) on the transport properties of silica hydrogels synthesized by TAFR. In all cases, the hydrogels have an amorphous structure that is characterized using small-angle X-ray scattering (SAXS) [28]. From the resulting data, it is shown that there is a clear correlation between the parameters describing the microstructure of the matrix and the transport of dye molecules, explaining non-monotonic changes in macroscopic properties for samples synthesized at pH values close to the pH corresponding to the minimum gelation time pH_{min}. This approach should contribute to the design of a rational synthesis pathway for a wide range of envisaged applications which demand the development of biocompatible materials with tuned transport properties.

2 Materials and methods

2.1 Silica hydrogel synthesis

TEOS (Aldrich) was employed as silica precursor, following the alcohol-free procedure [20]. Briefly, a silica sol stock solution was prepared by mixing 5.58 mL of tetraethoxysilane (TEOS, from Sigma-Aldrich), 1.9 mL of water and 0.125 mL of HCl 0.62 M. The mixture was stirred vigorously to obtain a homogeneous solution (i.e., to completeness of the hydrolysis reaction). This solution was diluted (50 % in water), and then the alcohol content was removed (up to ~98 %) by rotavapor methods with controlled vacuum (20 mbar) and low temperature (40 °C). Different volumes of silica sol stock and phosphate buffer solutions (0.1 M, pH between 6 and 8) were mixed to obtain silica content between 3.6 and 9.0 % in the final hydrogel samples, condensed at pH between 4.5 and 7.5. Condensation reaction was carried out at room temperature (20 °C), and all samples were aged in their mother liquors for at least 3 times of gelation (the time of gelation is highly dependent on the pH of synthesis) [24].

2.2 Transport properties

Evaluation of transport properties of cationic dye crystal violet (CV) through the silica hydrogels is performed on samples aged 24 h in phosphate buffer (pH 6.5, 0.1 M), at which the silica surface is negatively charged (isoelectric

point of silica ~pH 2). The monitoring of the transport of dyes was based on the digital analysis of images, as previously done [27]. The boundary conditions for one-dimensional diffusion were satisfied by seeding the dye on top of the monolithic hydrogels synthesized in plastic UV–visible cuvettes, and samples were immediately placed on a digital scanner to acquire images of dye concentration profile at different times by sequential scanning. Color intensity profiles at each time were obtained by image analysis with ImageJ free software [29].

The transport though these hydrogels is a complex process, where diffusion is coupled with adsorption on silica surface. Considering the diffusion of the dye through the aqueous pores, the effective diffusion coefficient (D_{eff}) is defined as

$$D_{\text{eff}} = D_{\text{aq}} \frac{\phi \delta}{\tau} \tag{1}$$

where D_{aq} is the diffusion coefficient of the dye in water, ϕ is the pore volume fraction, δ the constrictivity, and τ the tortuosity of the matrix.

To take into account the adsorption on silica surface, for the simplest model of a linear adsorption isotherm the concentration A of the dye immobilized by adsorption is directly proportional to the concentration C of dye free to diffuse, being R the partition constant:

$$A = RC \tag{2}$$

And then, the equation for diffusion in one dimension is modified as:

$$\frac{\partial C}{\partial t} = D_{\text{eff}} \frac{\partial^2 C}{\partial x^2} - \frac{\partial A}{\partial t} \tag{3}$$

From Eqs. 1 and 2, the usual form of the Fick equation is obtained for an apparent diffusion coefficient D_{app} given by $D_{\text{eff}}/(R + 1)$.

$$\frac{\partial C}{\partial t} = \frac{D_{\text{eff}}}{R+1} \frac{\partial^2 C}{\partial x^2} \tag{4}$$

For a punctual source and assuming semi-infinite conditions (i.e., the dye does not reach the other side of the diffusing matrix throughout the whole time of the experiment), the diffusion profile is given by Eq. 1, where M is the initial amount of dye seeded [30]:

$$C(x,t) = \frac{M}{\sqrt{\pi D_{\text{app}} t}} e^{\frac{-x^2}{4D_{\text{app}} t}} \tag{5}$$

This method allows the modeling of the cationic dye CV transport through the matrix, where the process of diffusion is coupled with the adsorption on the silica surface, in terms of an apparent diffusion coefficient (D_{app}) of the dye that accounts for the partition of the dye between solution and silica surface.

2.3 SAXS characterization of the microstructure

The microstructure characterization was performed at the LNLS SAXS2 beamline in Campinas, Brazil, working at $\lambda = 0.1488$ nm, wave vector range: $0.09\ \text{nm}^{-1} < q < 2.2\ \text{nm}^{-1}$ and a sample stage in vacuum with mica windows (standard for liquids) [31]. Data analysis was performed with SASfit program. Particulate silica hydrogels can be modeled as a fractal system although the rigorous interpretation of experimental results as indicating "fractality" requires many orders of magnitude of power-law scaling [32, 33]. The fractal dimension (D) and the radius of gyration of the primary cluster (R_{g}) were evaluated in terms of a mass fractal aggregation model, with an autocorrelation function of the form

$$g(r) \approx r^{D-d} h(r, \xi) \tag{6}$$

where d is the spatial dimension and the exponential cutoff function h describes the perimeter of the aggregate [34]. The parameter ξ is a cutoff length for the fractal correlations, proportional to the radius of gyration (R_{g}).

$$h = \exp\left[-\frac{r}{\xi}\right] \tag{7}$$

$$\xi^2 = \frac{2R_{\text{g}}^2}{D(D+1)} \tag{8}$$

The values of the parameter a (mean diameter of the elementary particles composing the structure) are obtained from the scattering curves from the q value corresponding to the intersection of the fit calculated for the experimental curve in the power-law region and the linear fit of the Porod region (at large q).

Considering a sharp interface between silica particles and aqueous pores, a parameter S related to the interfacial area can be derived from the asymptote of the scattering intensity $I(q)q^4$ versus q for large scattering wavenumbers q:

$$I(q)q^4 \sim S \tag{9}$$

Further information regarding the analysis of data can be found in Supplementary Information.

3 Results and discussion

Since hydrolysis and condensation processes occur separately, the hydrolysis conditions were identical for all the prepared samples, while the pH of condensation was varied from 4.5 to 7.5. The log–log SAXS intensity plots of TAFR hydrogels are indicative of scattering from a mass fractal system (see Figures SI-1 and SI-2 in Supplementary Information), as is frequently observed for

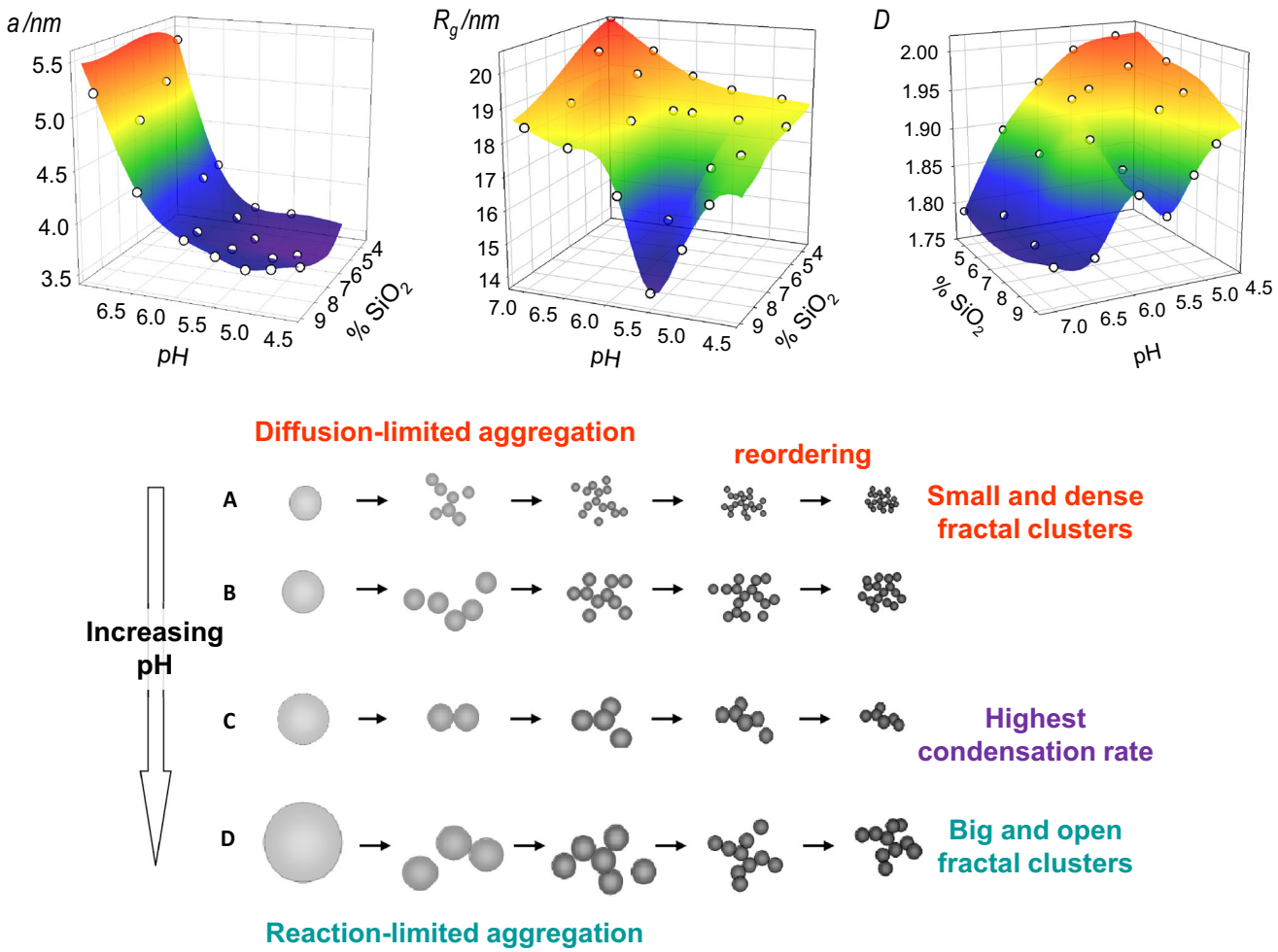

Fig. 1 Effect of the pH of the condensation reaction on the microstructure of the primary clusters. *Above* is shown the evolution of microstructure parameters a (mean diameter of elementary particles composing the structure), R_g (radius of gyration of primary clusters) and D (fractal dimension of the clusters) as derived from SAXS curves analysis. *Below* is presented a schematic representation of cluster formation during sol–gel synthesis at different pH conditions. Situation C represents the pH value that corresponds to the minimum gelation time (with a high condensation rate and intermediate particle size) for which a local minimum of D and R_g is observed

silica gels [35]. Figure 1 shows the evolution of the microstructure parameters derived from SAXS curves fitting for hydrogels with different total silica content (3.6–9.0 %). Fractal dimension (D), average cluster size (R_g) and mean diameter of the elementary particles composing the structure (a) are in good agreement with previous observations [24]. However, a more detailed study reveals that for higher silica concentrations anomalous values of parameters D and R_g are detected when working at a pH close to that of the minimum gelation time (pH_{min}). This range of pH close to neutrality has a great technological interest because it is close to the physiological pH of most relevant species used in biomaterial's applications and thus the highest viability is obtained when performing encapsulation procedures within this pH range (5.5–6.0).

The evolution of the microstructure parameters a, R_g and D with the silica concentration and pH of condensation is shown above in Fig. 1. The parameter a keeps approximately constant at low pH values (schematized below by situations A and B) and increases strongly with the pH of the condensation reaction for pH higher than pH_{min} (situations C, D). The attachment of particles to form clusters is also dependent on the pH of the condensation stage. Since the surface of silica is negatively charged above the isoelectric point (pH $\sim$ 2), the higher the pH of synthesis, the stronger the electrostatic repulsion between the particles. On the other hand, as the condensation reaction is catalyzed by OH^- groups, a higher pH increases the rate of reaction. As appreciated from the parameters derived from SAXS analysis, in a general trend, smaller and denser structures are obtained at low pH (i.e., with lower R_g and

higher D). This is due to the small size of elementary particles and the low electrostatic repulsion that allows particles to attach initially by weak interactions and reorder later into denser arrangements as condensation reaction occurs (situation A in schematic representation). Increasing the pH, the slight increase in particle size and the growing surface charge contribute to form more opened structures with a higher R_g (situation B). At pH values higher than pH_{min}, the huge electrostatic repulsion gives as a result even more opened structures (lower D) with an even higher R_g due mainly to a bigger particle size (D). However, the SAXS analysis shows that in the immediacy of pH_{min} for samples at high precursors' concentration, this trend is not followed: Inconsistent low values of D and R_g are obtained for samples at a silica concentration higher than 7.2 %. This can be interpreted as at the pH_{min}, the rate of condensation reaction significantly increases (being this effect more notorious for high silica concentration conditions), but the electrostatic repulsion slightly augments with pH. As a result, at the pH_{min} the frequency of fruitful particle collisions rises enormously, increasing the number of incipient clusters and decreasing the average number of particles forming the primary structure (represented in the scheme as situation C). As a whole, this results in extraordinary low D and R_g at pH values very close to the pH_{min}. Further increase in pH entails an important growth in particle size and a higher electrostatic repulsion that lowers the fraction of fruitful particle collisions, continuing with the general trend.

Within a general approach, in these mesoporous systems, mass transport involves at least two processes: diffusion and adsorption [36, 37]. The last one is particularly important in silica hydrogels due to the high specific surface area, hydrophilicity and surface charge on pore walls (isoelectric point of silica pH $\sim$ 2) [38]. In this context, the microstructure of samples plays a fundamental role in determining the apparent diffusion, which can be retarded by adsorption by a factor of $\sim$100 [39, 40]. To analyze the modulation of effective transport properties with synthesis conditions (pH of condensation and total silica content of samples), diffusion profiles of the probe crystal violet (CV) taken at different times were fitted to Fick diffusion model (see Sect. 2). Data obtained after 60, 120 and 300 min of dye seeding in one representative set of hydrogel samples (silica content of 3.6 %, synthesized at different pH in the range 5.4–6.6) are shown above in Fig. 2. For each sample, the diffusion profiles at all times essayed can be fitted with the same D_{app} (for the hydrogel samples shown in the figure, $D_{app} = 4.8 \times 10^{-12}$ m^2 s^{-1}, 3.2×10^{-12} m^2 s^{-1}, 6.1×10^{-12} m^2 s^{-1}, and 1.2×10^{-11} m^2 s^{-1}, for hydrogels synthesized at pH 5.4, 6.0, 6.3 and 6.6, respectively). Below in Fig. 2, the variation of D_{app} with both pH of condensation and total silica content is shown. For each set of samples with the same total silica content, D_{app} presents a local minimum at a pH $\sim$ 6. In a previous work where we analyzed the correlation between microstructure and optical properties of these systems [24], we found that the attenuance in the visible region showed a change in behavior at the pH of the minimum gelation time, pH_{min}. For all silica concentrations analyzed (3.6–10.7 %), a local maximum of attenuance was evidenced in the immediacy of the corresponding pH_{min}. This last value, essayed independently, slightly changed from 6.0 for hydrogels with the lowest silica content to 5.5 for hydrogels with the highest silica content [24]. Similarly, in this study pH_{min} values agree with a local minimum in D_{app}.

It is important to notice that these microstructure parameters individually do not present any simple relation with porosity or specific surface area of the hydrogel samples, and so transport properties of these samples cannot be predicted from them. However, dealing with Euclidean particles (i.e., in the region in which it is valid the Porod approximation), a plotting of SAXS intensity multiplied by the modulus of the scattering vector raised to the fourth, $I(q)\cdot q^4$, as a function of the modulus of scattering vector, q, tends to a constant value. This constant value (hereinafter referred to as parameter S) is related to the specific surface area of the hydrogel samples (see Figure SI-2 in Supplementary Information).

Figure 3 presents the evolution of the parameter S with silica concentration and the pH of condensation. The inset of the figure illustrates the plotting of $I(q)\cdot q^4$ versus q for a particular set of hydrogels (with silica content = 7.2 %). As a general trend, it can be seen that a lower value of parameter S is obtained by increasing the pH of silica condensation, which can be explained as a consequence of a higher particle size (parameter a, Fig. 1). However, for samples with high silica concentration, an anomalous behavior is observed near pH_{min}, where parameter S reaches a maximum. Comparing the values of D_{app} and S in Figs. 2 and 3, respectively, it becomes evident that the range of pH/silica concentrations that show slow mass transport coincide with that for which parameter S is maximum (i.e., hydrogels with high silica content, synthesized at pH $\sim$ pH_{min}).

To further analyze the correlation between microstructure and transport properties, the dependence of D_{app} on the reciprocal of parameter S for each set of samples with different silica concentrations is shown in Fig. 4. In good agreement with previous results [40], for each silica concentration D_{app} was found to be directly proportional to the reciprocal of parameter S, a measure of specific surface area of hydrogel samples. Moreover, when evaluating the slope of each linear regression as a function of silica concentration, we found that they are highly correlated. It is important to notice that the pore volume fraction, ϕ, the

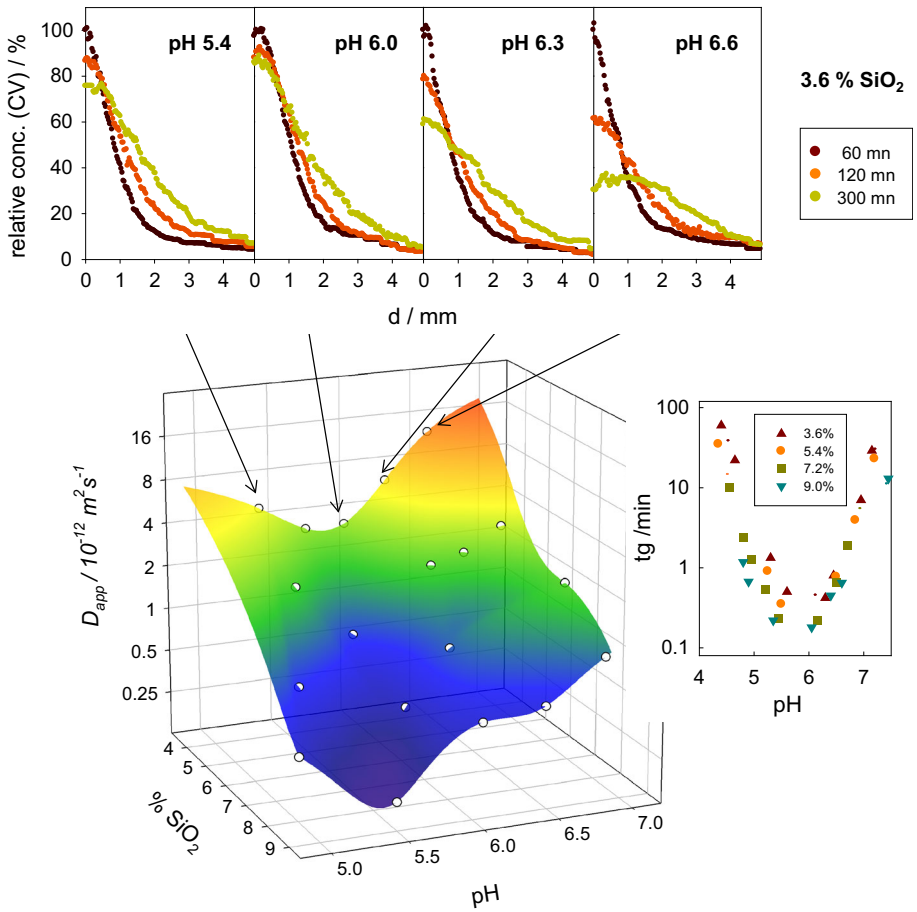

Fig. 2 Apparent diffusion coefficient (D_{app}) of cationic dye crystal violet (CV). *Above*: CV diffusion profiles taken at different times (60, 120 and 300 min) for samples with 3.6 % total silica concentration synthesized at the specified pHs. *Below*: D_{app} as a function of total silica content and pH of condensation. For each set of samples with the same total silica concentration, D_{app} presents a local minimum at a pH $\sim$ 6, which coincides with the pH of the minimum gelation time (pH_{min}), shown in the *inset*

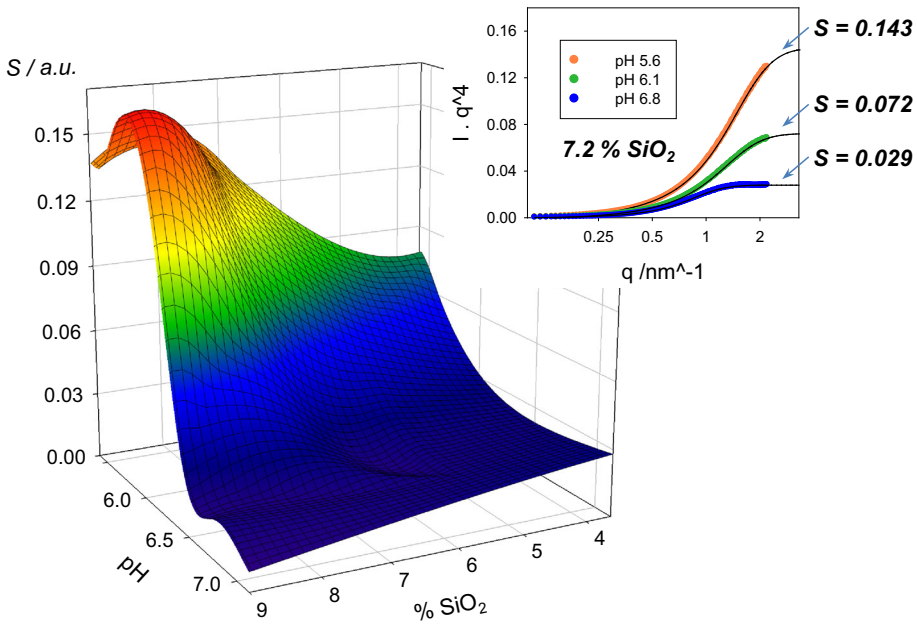

Fig. 3 Parameter S (in arbitrary units), related to the specific surface area, as a function of silica concentration and the pH of condensation of samples. The *inset* of the figure illustrates the plotting of $I(q)\cdot q^4$ versus q for a particular set of hydrogels (with silica content = 7.2 %), and the parameter S is derived from the constant value of this function at high q

constrictivity, δ, and the tortuosity, τ, of the matrix significantly change for each silica total content, and thus a simple relation between the slope of D_{app} versus S^{-1} and silica total content is not expected. However, an empirical exponential decay was observed. This goes to show that there is a high correlation between the microstructure of

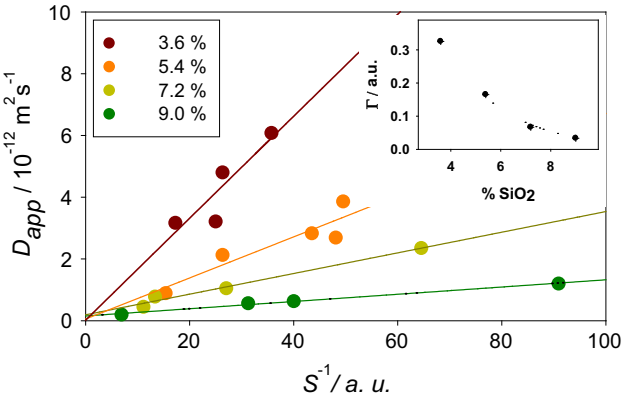

Fig. 4 Dependence of the apparent diffusion coefficient (D_{app}) on the reciprocal of parameter S for each set of samples with different silica total content: 3.6–9.0 % of SiO_2, as indicated. In all cases a direct proportionality is evidenced. The *inset* of the figure shows the dependence of the slope ($\Gamma = D_{app} \cdot S$) with the silica concentration of samples (exponential decay)

gels as evaluated from SAXS experiments and the transport of positively charged probes though these samples.

4 Conclusions

The transport properties of the hydrogels as any other macroscopic property are determined by the microstructure of the samples. Here we analyze the dependence of the apparent diffusion coefficient D_{app} on both the total silica content and the pH of condensation of silica matrices, and the correlation between transport properties and the microstructure of the hydrogel samples. D_{app} reflects the interaction of the dye with silica surface and allows modeling the transport process in these matrices for many potential applications, such as drug delivery or biosensors that need to finely regulate the transport of a biomolecule of interest.

These results, which were obtained for a wide pH and silica concentration range, reinforce the idea that the behavior of gels determined in a restricted interval of synthesis variables cannot be extrapolated, as at pH values close to those corresponding to the minimum gelation time, non-monotonic changes both in microstructure parameters and in transport properties are observed. On the other hand, effective transport properties were found to be highly correlated to the surface area derived from SAXS analysis of samples' microstructure, revealing that this macroscopic property can be easily predicted from SAXS analysis, in particular around neutral pH that is relevant for biotechnological applications. And vice versa, simple experiments of dye diffusion can give valuable information about the microstructure of these systems, which is even more important from a practical point of view. In conclusion, in this work we show that a simple experiment of dye diffusion can give valuable insight into the transport processes, being a powerful tool for the rational design of applications that require the tuning of transport properties.

Acknowledgments This work has been supported by the Brazilian Synchrotron Light Laboratory (LNLS, Brazil, Proposal D11A-SAXS-6039), the University of Buenos Aires (UBACyT 20020130100048BA), and by Agencia Nacional de Promoción Científica y Tecnológica (ANPCyT PICT 2013-2045 and 2012-1167). S.A.B., M.J. and M.P. are Research Scientists of CONICET (Argentina).

References

1. Avnir D, Lev O, Livage J (2006) Recent bio-applications of sol–gel materials. J Mater Chem 16(11):1013–1030
2. Livage J, Coradin T (2006) Living cells in oxide glasses. Rev Miner Geochem 64(1):315–332
3. Meunier CF, Dandoy P, Su B-L (2010) Encapsulation of cells within silica matrixes: towards a new advance in the conception of living hybrid materials. J Colloid Interface Sci 342:211
4. Perullini M, Orias F, Durrieu C, Jobbágy M, Bilmes SA (2014) Co-encapsulation of *Daphnia magna* and microalgae in silica matrices, a stepping stone toward a portable microcosm. Biotechnol Rep 4:147–150
5. Pannier A, Soltmann U, Soltmann B, Altenburger R, Schmitt-Jansen M (2014) Alginate/silica hybrid materials for immobilization of green microalgae *Chlorella vulgaris* for cell-based sensor arrays. J Mater Chem B 2:7896–7909
6. Ge X, Eleftheriou NM, Dahoumane SiA, Brennan JD (2013) Sol–gel-derived materials for production of pin-printed reporter gene living-cell microarrays. Anal Chem 85:12108–12117
7. Brayner R, Couté A, Livage J, Perrette C, Sicard C (2013) Microalgal biosensors. Anal Bioanal Chem 401(2):581–597
8. Perullini M, Ferro Y, Durrieu C, Jobbagy M, Bilmes SA (2014) Sol gel silica platforms for microalgae-based optical biosensors. J Biotechnol 179(1):65–70
9. Perullini M, Rivero MM, Jobbagy M, Mentaberry A, Blimes SA (2007) Plant cell proliferation inside an inorganic host. J Biotechnol 127(3):542–548
10. Nassif N, Roux C, Coradin T, Bouvet OMM, Livage J (2004) Bacteria quorum sensing in silica matrices. J Mater Chem 14(14):2264–2268
11. Fiedler D, Hager U, Franke H, Soltmann U, Böttcher H (2007) Algae biocers: astaxanthin formation in sol–gel immobilised living microalgae. J Mater Chem 17(3):261–266
12. Soler-Illia GJAA, Innocenzi P (2006) Mesoporous hybrid thin films: the physics and chemistry beneath. Chem Eur J 12:4478–4494
13. Otal EH, Angelomé PC, Bilmes SA, Soler-Illia GJAA (2006) Functionalised mesoporous hybrid thin films as selective membranes. Adv Mater 18:934–938
14. Collard X, Van der Schueren B, Rooke J, Aprile C, Su B (2013) A comprehensive study of the reaction parameters involved in the synthesis of Silica thin films with well-ordered uni-directional mesopores. J Colloid Interface Sci 401:23–33
15. Perullini M, Jobbágy M, Moretti MB, Correa García S, Bilmes SA (2008) Optimizing silica encapsulation of living cells. In situ evaluation of cellular stress. Chem Mater 20:3015–3021

16. Kuncova G, Podrazky O, Ripp S, Trögl J, Sayler GS, Demnerova K, Vankova R (2004) Monitoring of the viability of cells immobilized by sol–gel process. J Sol-Gel Sci Technol 31:1–8
17. Perchacz M, Benes H, Kobera L, Walterova Z (2015) Influence of sol–gel conditions on the final structure of silica-based precursors. J Sol-Gel Sci Technol 75:649–663
18. Reichenauer G (2004) Thermal aging of silica gels in water. J Non-Cryst Solids 350:189–195
19. Coiffier A, Coradin T, Roux C, Bouvet OM, Livage J (2001) Sol–gel encapsulation of bacteria: a comparison between alkoxide and aqueous routes. J Mater Chem 11:2039–2044
20. Ferrer ML, Del Monte F, Levy D (2002) A novel and simple alcohol-free sol-gel route for encapsulation of labile proteins. Chem Mater 14:3619–3621
21. Ferrer ML, Yuste L, Rojo F, Del Monte F (2003) Biocompatible sol–gel route for encapsulation of living bacteria in organically modified silica matrixes. Chem Mater 15:3614–3618
22. Himmel B, Gerberb Th, Bürger H (1990) WAXS- and SAXS-investigations of structure formation in alcoholic SiO2 solutions. J Non-Cryst Solids 119:1–13
23. Mandelbrot BB (1983) The fractal geometry of nature. Freeman, San Francisco
24. Perullini M, Jobbagy M, Bilmes SA, Torriani IL, Candal R (2011) Effect of synthesis conditions on the microstructure of TEOS derived silica hydrogels synthesized by the alcohol-free sol–gel route. J Sol-Gel Sci Technol 59(1):174–180
25. Tantemsapya N, Meegoda JN (2004) Estimation of diffusion coefficient of chromium in colloidal silica using digital photography. Environ Sci Technol 38:3950–3957
26. Ray E, Bunton P, Pojman JA (2007) Determination of the diffusion coefficient between corn syrup and distilled water using a digital camera. Am J Phys 75:903–906
27. Perullini M, Jobbágy M, Japas ML, Bilmes SA (2014) Simultaneous determination of diffusion and adsorption of dyes in silica hydrogels. J Colloid Interface Sci 425:91–95
28. Schmidt PW, Höhr A, Neumann H-B, Kaiser H, Avnir D, Lin JS (1989) Small angle X-ray scattering study of the fractal morphology of porous silicas. J Chem Phys 90(9):5016–5023
29. http://rsb.info.nih.gov/ij/download.html
30. Crank J (1975) The mathematics of diffusion, 2nd edn. Clarendon Press, Oxford
31. Cavalcanti LP, Torriani IL, Plivelic TS, Oliveira CLP, Kellermann G, Neuenschwander R (2004) Rev Sci Instrum 75:4541
32. Schaefer DW, Keefer KD (1984) Fractal geometry of sílica condensation polymers. Phys Rev Lett 53(14):1383–1386
33. Avnir D, Biham O, Lidar D, Malcai O (1998) Is the geometry of nature fractal? Science 279:39–40
34. Sorensen CM, Wang GM (1999) Size distribution effect on the power law regime of the structure factor of fractal aggregates. Phys Rev E 60(6):7143–7148
35. Vinogradova E, Moreno A, Lara VH, Bosch P (2003) Multifractal imaging and structural investigation of silica hydrogels and aerogels. Silicon Chem 2:247–254
36. Ruthven DM (2004) Sorption kinetics for diffusion-controlled systems with a strongly concentration-dependent diffusivity. Chem Eng Sci 59:4531–4545
37. Ruthven DM (1984) Principles of adsorption and adsorption processes. Wiley, New York
38. Alexander F, Poots VJP, McKay G (1978) Adsorption kinetics and diffusional mass transfer processes during colour removal from effluents using silica. Ing Eng Chem Process Des Dev 17(4):406–410
39. Perullini M, Calcabrini M, Jobbágy M, Bilmes SA (2015) Alginate/porous silica matrices for the encapsulation of living organisms: tunable properties for biosensors, modular bioreactors, and bioremediation devices. Mesoporous Biomater 2:3–12
40. Perullini M, Amoura M, Roux C, Coradin T, Livage J, Japas ML, Jobbagy M, Bilmes SA (2011) Improving silica matrices for encapsulation of *Escherichia coli* using osmoprotectors. J Mater Chem 21:4546